A Study Of Aerodynamic Characteristics Of S-Shaped Savonious Rotor With Different Number Of Blades

Rumana Hossain
Department of Physical science, Independent University, Bangladesh

Shaukat Ahmed
Department of Industrial and Production Engineering, BUET

Abstract

The S-shaped rotor is a modification of the Savonius rotor with no overlap. In this paper the drag and torque coefficients of stationary S-shaped two, three, four bladed rotor have been investigated by measuring the pressure distribution on the blade surfaces for various rotor angles. The experiments have been carried out at Reynolds number $1.1*10^5$ in a uniform flow jet produced by an open circuit wind tunnel. The measurements indicate that drag force and so that the torque, varies with rotor angle. The results facilitate predicting the performance of these types of rotor under dynamic conditions. It is experimentally obtain that if the number of blade is increased there is no significant change in the tangential drag co-efficient but the starting torque increases drastically due to the increase of pressure difference and hence the normal force acting on the rotor blade.

Keywords: S-shaped Savonius rotor, Drag co-efficient, Torque co-efficient

1. Introduction

The wind is an inexhaustible source of energy. In fact it can be regarded as an indirect form of solar energy, the movements of the atmosphere resulting as they do from the intermittent heating effects of the sun's radiation on the air itself and on the earth and the sea. The wind is provided mechanical power for pumping water and for milling grain through many centuries, and continues to serve as the electrical power source of many thousands of homesteads and farms in the rural areas.

Throughout history people have harnessed the wind. More than 5000 years ago, the Egyptians used the wind to sail ships on the Nile. Later, people built the first turbines to grind grain. These machines looked like paddle wheels and were used in Persia as early as 200 B.C. By the 14th century, the Dutch had taken the lead in improving the design of windmills. They invented propeller type blades and used wind power to drain the marshes and lakes of the Rhone River delta. In America, early European settlers used windmills to grind wheat and corn, to pump water, and to cut wood at sawmills. By the early twentieth century, small windmills were used for pumping water and electric power generation in Europe, the United States, Africa, and elsewhere. In addition to thousands of small wind electric generators, a few larger systems were built in North America and Europe. In the 1970's, increases in the price of oil and other fossil fuels helped wind power return as an economically viable, alternative source of energy. Governments all over the world, especially in North America and Europe, instituted research and development programs. These efforts led to the development of modern wind turbines, which have dramatically reduced the cost of generating electricity from wind power. As a result, wind energy contributed 3.8 billion kilowatt-hours of electricity in 1991, enough to power more than 500,000 households.

Blowing wind spins the blades on a wind turbine just like a large toy pinwheel. The blades are attached to a hub that is mounted on a turning shaft. The shaft goes through a gear transmission box where the turning speed is increased. The transmission is attached to a high speed shaft which turns a generator that makes electricity. If the wind gets too high, the turbine has a brake that will keep the blades from turning and being damaged.

Modern wind turbines are divided into two major categories: horizontal axis turbines and vertical axis turbines. Horizontal axis turbines are the most common turbine configuration used today. They consist of a tall tower, atop which sits a fan-like rotor that faces into or away from the wind, the generator, the controller, and other components.

Most horizontal axis turbines built today are two- or three-bladed, although some have fewer or more blades. Vertical axis turbines fall into two major categories: Savonius and Darrieus. Neither turbine type is in wide use today.

The Darrieus turbine was invented in France in the 1920s. Often described as looking like an eggbeater, this vertical axis turbine has vertical blades that rotate into and out of the wind. Using aerodynamic lift, these turbines can capture more energy than drag devices. The Giromill and cycloturbine are variants on the Darrieus turbine [4].

First invented in Finland, the Savonius turbine is S-shaped if viewed from above. This drag-type VAWT turns relatively slowly, but yields a high torque. It is useful for grinding grain, pumping water, and many other tasks, but its slow rotational speeds are not good for generating electricity [4].

The cost of energy from the wind has dropped by 85% during the last 20 years. Incentives like the federal production tax credit and net metering provisions available in some areas improve the economics of wind energy. The rate the utility pays to purchase wind-generated electricity, called the buy-back rate, often determines the economic feasibility of a project. Wind energy is often attractive when life-cycle costs are compared with other generation technologies. With utility deregulation, wind energy may be impacted by added costs for ancillary services, the support services needed to generate and deliver electricity.

2. Literature Review

From the ancient period people have been working on various types of wind turbine to extract energy. However, expected developments have not been achieved in wind driven machines to cope with the characteristics of wind turbines. Conventional machines are being used now-a-days even though they are not always suitable from the operational point of view. Wind turbines in ancient period were of drag types only and their efficiencies were not up to the mark. Arising from the increasing practical importance of wind turbine aerodynamics, there have been, over the past few decades, and enormous increase in research works concerning laboratory simulations, full scale measurements and more recently, numerical calculations and theoretical predictions of flows over a wide variety of Savonius rotors. Researchers in different countries have been contributing greatly to the knowledge of analytical prediction methods of wind turbines, but the major part of the reported works have been of fundamental nature involving the flow over horizontal axis wind turbine and vertical axis Darrieus rotor. The primary attraction of the vertical axis wind turbine is the simplicity of its manufacture compared to the horizontal axis wind turbine. Most of the researchers have concluded research work on S-shaped rotor with various flow parameters.

Islam et al. [5] investigated that the aerodynamic forces acting on a stationary S-shaped rotor and made an attempt to predict the dynamic performance from these forces. The work was done by measuring the pressure distribution over the surfaces of the blades. The measurements were carried out in a uniform flow jet produced by an open circuit wind tunnel and at a constant wind speed of 8.9 m/s which corresponds to a Reynolds number of $1.13*10^5$.
The results indicate that flow separates over the front and back surfaces of the blades and the point of separation depends on the rotor angle. The pressure difference was observed between the convex and concave surfaces of each blade, which in turn gave drag coefficients. The drag and hence, the torque of each blade varies with rotor angle and was found to be maximum at $\alpha=45^0$ for the advancing blade and at $\alpha=45^0$ for the returning blade. The maximum net torque was obtained at $\alpha=45^0$ and became negative in the range of rotor angle between135^0 to 165^0.

Islam et al. [6] analyzed the performance of S-shape rotor by placing a flat plate in front of the returning blade. They found that the power coefficient of the S-rotor was dependent on the Reynolds number. The value of Cp (power coefficient) increased with Reynolds number in the range of the Reynolds number studied and a maximum of 20% of power coefficient was increased by using the deflecting plate which occurred at a deflecting angle of 35^0 for b=0.5D, where b=distance between plate and rotor center and D=diameter of the rotor.

There are several variations of Savonius rotor. The efficiency of a Savonius is only around 15 % but they are ideal for many situations. They will start spinning with very little wind, produce a great amount of torque, and need no speed limiter. The Savonius rotor is designed for low RPM applications, and will never spin faster than the speed of the wind. Some variations are shown below, looking down from the top of the turbine.

3. Details of Non-Dimensional Parameters

In this project, the local surface pressures on the blade surfaces of the rotor were measured relative to the free upstream static pressure prevailing in the test section of the wind tunnel. The data obtained experimentally have been presented in terms of

non-dimensional coefficients. The equations of coefficient of pressure, normal and tangential drag co-efficient and torque coefficient are briefly described in this section.

3.1 Static Aerodynamic Characteristics

In the following two steps the procedure for calculating the static aerodynamic characteristics is mentioned:

Step1: From the experimental data pressure coefficients both for concave and convex surfaces of blades are calculated for angle of rotation ranging from 0^0 to 340^0.

Step2: The flow pattern produced by the rotor blades is characterized by high turbulence, unsteadiness and flow separation. The combined effect of these flow features in turn produces pressure differences between the concave and convex surfaces of the blades. These pressure differences result in aerodynamic forces and hence torques. These forces can be resolved into components F_n and F_t along normal and tangential directions of the rotor chord.

3.1.1 Pressure Coefficient, C_p

In the experiment, the pressure measurements were made at 8 tapping points on each blade for the angle of rotation (α) at every 20^0 interval ranging from 0^0 to 340^0 on both concave and convex surfaces. Using these raw data pressures, coefficient on convex and concave surfaces of the blades are measured by the following equation:

$$C_P = \frac{P - P_0}{1/2\rho U_0^2}$$

Where, $P\text{-}P_0$ = Difference between blade and atmospheric pressure. ρ = Density of air. U_0 = Free stream velocity.

3.1.2 Drag Coefficients

These pressure differences between the concave and convex surfaces of the blades result inaerodynamic forces and hence torques. These forces can be resolved into components F_n and F_t along normal and tangential directions of the rotor chord as shown in Figure 1.

The corresponding drag coefficients can be expressed as

$$C_{n_i} = \frac{F_{n_i}}{1/2\rho U_0^2 R};\ C_{t_i} = \frac{F_{t_i}}{1/2\rho U_0^2 R}$$

Where subscript i indicates the pressure tapping number.

The forces F_n and F_t can be evaluated from the pressure differences as

$$F_{n_i} = \Delta P_i \Delta S_i \sin\phi_i;\ F_{n_i} = \Delta P_i \Delta S_i \cos\phi_i$$

Where ΔP_i is the pressure difference between the concave and convex surfaces of the blade at a particular pressure tapping i, ΔS_i is the chord length around the tapping i, where a uniform pressure is assumed

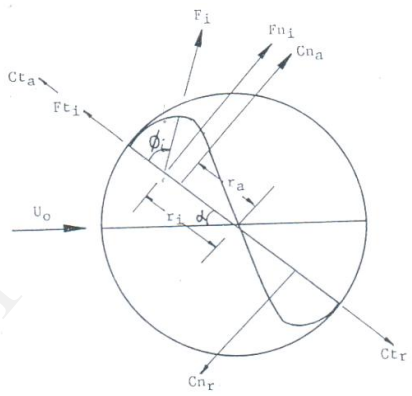

Figure 1. Forces acting on rotor blades

3.1.3 Torque Co-efficient

The normal force is responsible for producing a torque on the rotor shaft and this torque can be expressed for an element of the blade as

$$T_i = F_{n_i} r_i$$

Torque coefficient can be written as

$$C_{q_i} = \frac{T_i}{1/2\rho U_0^2 RR/2}$$

Total drag coefficient and torque coefficient for an individual plate at a particular rotor angle, α are evaluated by integrating the coefficients over the blade surfaces. Then

$$C_n(\alpha) = \sum_{i=1}^{8} C_{n_i} \; ;$$

$$C_t(\alpha) = \sum_{i=1}^{8} C_{t_i} \; ;$$

$$C_q(\alpha) = \sum_{i=1}^{8} C_{q_i}$$

4. Experimental Set-up and Procedure

The objectives of this project to investigate the effect of wind on the S-shaped four, three, and two bladed Savonius rotor have been performed with the help of a subsonic wind tunnel, experimental set-up of the Savonius rotors and an inclined multi manometer. Pressure distributions on the convex and concave surfaces of the blades of the S-shaped Savonius rotors placed normal to the approaching uniform flow have been measured with the help of the multi manometer. The following sections describe in detail about the experimental set-up and the techniques adopted for the investigation.

4.1 The Wind Tunnel

The open circuit subsonic wind tunnel is 6.55m long with a test section of (490mm×490mm) cross section. Figure depicts the wind tunnel used for the experiment. The successive sections of the wind tunnel comprise of converging mouth, Perspex section, rectangular section, fan section (two rotary axial flow fans), butterfly section, silencer with honey comb section, an eddy breaker, diverging section, converging section, 610 mm long rectangular section, 305 mm long flow straighter section and 610 mm long rectangular exit section. The central longitudinal axis of the wind tunnel has been maintained at a constant height from the floor.

The converging mouth entry has been incorporated into the system for easy entry of air into the tunnel and to maintain uniform flow into the duct free from outside disturbances. The exposed surface of the mouth entry has been covered with cloth for extra protection against dust and for uniform flow.

The Perspex section (305mm×305mm) is 610 mm long that may be used for the experiment of flow around the circular cylinder. A 920 mm long rectangular diverging section has been used to make the flow uniform from rotation.

The induced flow through the wind tunnel has been produced by a two stage rotating axial flow fan (Woods of Colchester Ltd., England, Type 38 JTE) of capacity 14.15 m^3/s at a head of 152.4 mm of water and 1475 rpm. A butterfly valve actuated by a screw thread mechanism has been placed behind the fan and used to control the flow. A silencer has been fitted at the end of the flow controlling section in order to reduce the noise of the system at the same time a flow straighter system has been used in this section.

The diverging and converging section of the wind tunnel is 460 mm long and made of 16 SWG black sheets. The angle of divergence and convergence is 7^0, which has been made with a view to minimize expansion and contraction loss and to reduce the possibility of flow separation. Other three square sections have been used to make the flow straight and uniform.

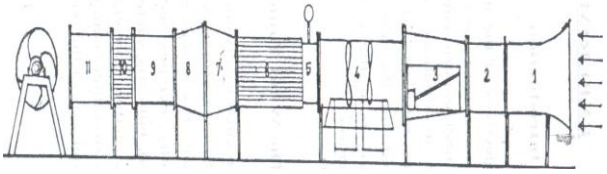

Figure 2. Schematic Diagram of Wind Tunnel

1. Converging Mouth Entry; 2. Perspex Section; 3. Rectangular Diverging Section; 4. Fan Section; 5. Butterfly Section; 6. Silencer with Honeycomb Section; 7. Diverging Section ; 8. Converging Section; 9. Rectangular Section; 10. Flow Straighter Section; 11. Rectangular Exit Section

4.2 Construction of the S-shaped Savonius rotor

The rotor blade design is geometrically identical to that detailed by Littler [1].The four, three, two bladed rotors are made up of four, three, two blades of chord length 91.44 mm each and height, H = 342.9 mm each. The blades are made of PVC material. Each rotor is fixed on an iron frame by using two side shafts and two ball bearings.

The pressure measuremenst have been made at 8 tapping points on any two blades of each rotor. The tapping are made with copper tubes that have been press fitted to the tapping holes. The tapping are located at the mid plane on one side of each blade, so that pressure at every 20^0 on the blade surface can be measured. The pressure tapping have been connected to an inclined multi-manometer (manometric fluid is water) through PVC tubes.

4.3 Experimental procedure

The flow velocity in the test section was kept constant at 8.7 m/s. The Reynolds number (Re = U0D/v) based on rotor diameter, D = 190.5mm was 1.07×105. The effect of the temperature was considered in this experiment and the experiment was carried at atmospheric temperature i.e, at

T=250C where the kinematic viscosity of air was 1.55×105 m^2/s. The Savonius rotor with frame was placed 500 mm upstream in front of the exit section of the wind tunnel. One blade of the rotor was fixed parallel to the free stream velocity i.e, parallel to horizontal, which was called the reference plane and from this plane, angle of rotation was measured. Then the first blade was kept at 00 angle of rotation, exposing the convex surface in front of the free stream of air, and other blades are kept at particular angles. The rotor was made static fixing one side of the shaft of the rotor with the angle-fixing device. Pressure on the convex surfaces of blades was measured at a particular rotor angle α, keeping the rotor static. Gradually pressure on the convex surfaces of blades was measured in this process for every 200 interval. The same steps were repeated for the measurement of pressure on concave surfaces. At a particular rotor angle α, the rotor blades had experienced forces due to pressure differences between the concave and convex surfaces, which were resolved into normal forces and tangential forces.

5. Results and Discussion

The pressure distributions over the surfaces of the blades are measured at every 80^0 interval of rotor angle for two, three and four bladed rotor. At a particular rotor angle α, the blades had experienced forces due to pressure differences between the concave and convex surfaces, which were resolved into normal and tangential forces. As mentioned earlier, the differences in pressure between the front and backside of the blade result drag forces in normal and tangential direction. Normal drag coefficients are plotted against different rotor angles in Figure 3.

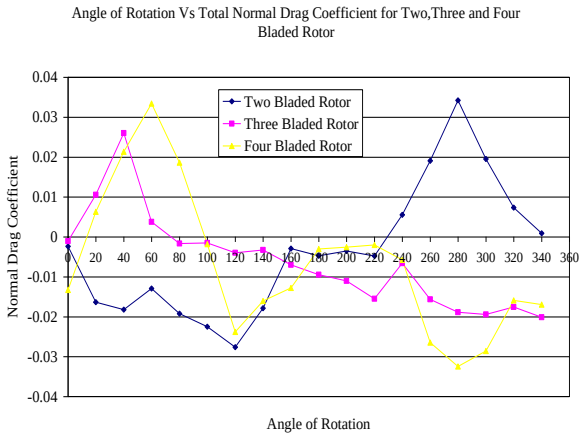

Figure 3. Variation of the Total Normal Drag Coefficient with the change of the Angle of Rotation for Two, Three and Four Bladed Rotor

In case of two bladed rotor C_n decreases from α=0° rotor angle up to α=120^0 in a fluctuating manner and after that it increases upto 160^o. From 160^0 to 220^0 it is almost constant and then increases abruptly up to 280^0 and then it decreases drastically. Minimum negative normal drag occurs at α= 120° and maximum positive occurs at rotor angle 280°. For the three bladed rotor the value of C_n starts increasing from the 0^0 and reaches its peak at α=40^0 then it decreases with fluctuation as the α increases. In case of four bladed rotor the value of C_n increases from α=0^0 to α=60^0 and it has the highest positive value at this point. Then it decreases abruptly up to α=120^0 and after that it starts increasing again up to α=180^0. From 180^0 to 220^0 of rotor angle it is almost constant. After α=220 normal drag co-efficient decreases up to α=280^0 and at that point it has the lowest negative value. After α=280^0 it starts increasing again up to 320^0. Overall the torque co-efficient shows a cyclical pattern in which decreases eventually for the four bladed rotor. Tangential drag coefficients are plotted against different rotor angles in Figure 4.

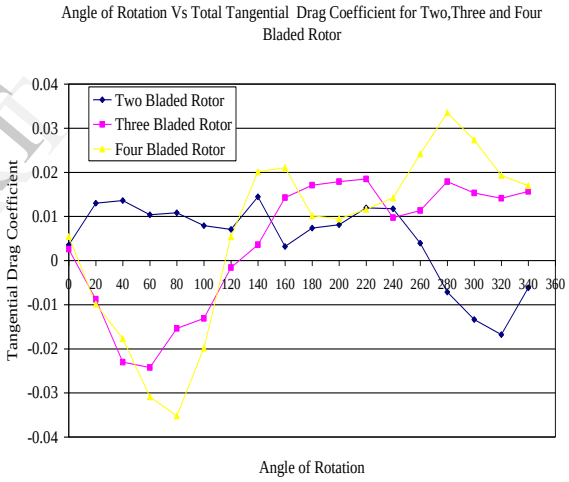

Figure 4. Variation of the Total Tangential Drag Coefficient with the change of the Angle of Rotation for Two, Three and Four Bladed Rotor

The tangential drag co-efficient in case of two bladed rotor the value of C_t fluctuates around 0.01 from 0^0 to 240^0 then it starts decreasing up to 320^0. For both the three and four bladed rotor it starts decreasing at first and reaches into the highest negative co-efficient and then it starts increasing in a fluctuating manner as the degrees increases.Torque drag coefficients are plotted against different rotor angles in Figure 5.

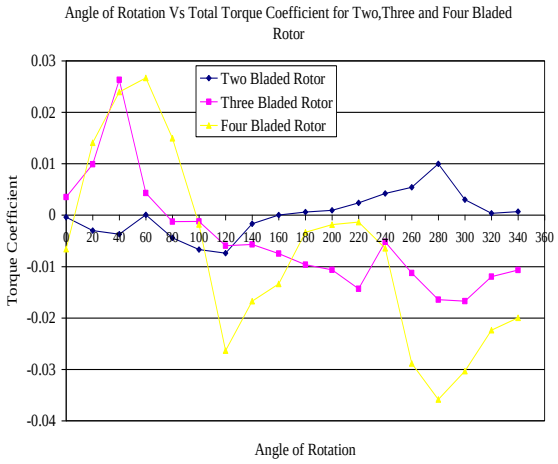

Figure 5. Variation of the Total Torque Coefficient with the change of the angle of rotation for Two, Three and Four Bladed Rotor

The torque co-efficient is fluctuating around the value of zero. It has the highest positive co-efficient at $\alpha=280^0$ and lowest negative co-efficient at $\alpha=120^o$. For the three bladed rotor the value of C_q starts increasing from the $\alpha=0^0$ and reaches the peak at $\alpha=40^0$. After that it decreases abruptly up to $\alpha=60^0$ and then it starts decreasing eventually in a fluctuating manner and does not touch the zero line. In case of four bladed rotor the value of C_q increases from $\alpha=0^0$ to $\alpha=60^0$ and it has the highest positive value at this point. Then it decreases drastically up to $\alpha=120^0$ and after that it starts increasing again up to $\alpha=220^0$. After $\alpha=220$ torque co-efficient decreases up to $\alpha=280^0$ and at that point it has the lowest negative value. After $\alpha=280^0$ it starts increasing again. Overall the torque co-efficient shows a cyclical pattern in decreasing manner for the four bladed rotor.

6. Conclusion

The present study concerns the pressure distributions over the two, three and four blades of the rotor on both the convex and concave surfaces at different angles of rotation. A pressure difference is obtained from the concave and convex surface, which in turn gives drag coefficients. The drag coefficients may be resolved along the normal and tangential directions of the rotor chord. The normal drag is responsible for the torque production. The drag and hence the torque of each blade varies with rotor angle. Further research is needed for studying the effects on the performance of an S-shape savonius rotor by placing guide vanes around the rotor. The effects of the shape and the number of guide vanes may also be studied.

Reference:

[1] Littler, R.D., Further theoretical and Experimental Investigation of the Savonius Rotor, B.E. Thesis, University of Queensland, Australia, 1975.
[2] Bowden, G. J. and McAleese, S.A., The properties of isolated and Coupled Savonius Rotors, *Wind Engineering*, vol. 8, no.4, UK, 1984.
[3] Islam, M.Q., Islam, A.K.M.S., and Nur, M.A, Aerodynamic characteristics of a stationary S-shaped Savonius Rotor, Dept of Mech. Engg., BUET.
[4] www.eere.energy.gov
[5] Islam, A.K.M.S., Islam, M.Q., Razzaque, M.M. and Ashraf . R.(1995), Static Torque and Drag Characteristics of an S-shaped Savonius rotor and Prediction of dynamic Characteristics, *Wind Engineeering*, vol. 19, no 6.
[6] Huda, M.D., Selim, M.A., Islam, A.K.M.S. and Islam, M.Q. (1992), The performance of an S-shaped Savonius Rotor with a Deflecting Plate, RERIC Int. *Energy Journal*, vol. 14 no. 1, pp. 25-32.
[7] Lysen, E.H., Bos, H.G and Cordes, E.H (1978), Savonius Rotors for Water Pumping, *SWD publication*, Amersfoort, The Netherlands.
[8] Islam, M.Q. and Hossain, M.A., Savonius Rotor for Lifting Water in Bangladesh, Mech. Engg. Res. Bull., Vol.4 (1981), No.1